

Article

Oxidoborates Templated by Cationic Nickel(II) Complexes and Self-Assembled from B(OH)₃

Mohammed A. Altahan ^{1,†}, Michael A. Beckett ^{1,*} , Simon J. Coles ²  and Peter N. Horton ²¹ School of Natural Sciences, Bangor University, Bangor LL57 2UW, UK; chs030@bangor.ac.uk² School of Chemistry, University of Southampton, Southampton SO17 1BJ, UK; S.J.Coles@soton.ac.uk (S.J.C.); P.N.Horton@soton.ac.uk (P.N.H.)

* Correspondence: m.a.beckett@bangor.ac.uk

† Current address: Chemistry Department, College of Science, University of Thi-Qar, Nasiryah 0096442, Iraq.

Abstract: Several oxidoborates, self-assembled from B(OH)₃ and templated by cationic Ni^(II) coordination compounds, were synthesized by crystallization from aqueous solution. These include the ionic compounds *trans*-[Ni(NH₃)₄(H₂O)₂][B₄O₅(OH)₄]·H₂O (**1**), *s*-[Ni(dien)₂][B₅O₆(OH)₄]₂ (dien = *N*-(2-aminoethyl)-1,2-ethanediamine (**2**), *trans*-[Ni(dmen)₂(H₂O)₂][B₅O₆(OH)₄]₂·2H₂O (dmen = *N,N*-dimethyl-1,2-diaminoethane (**3**), [Ni(HEen)₂][B₅O₆(OH)₄]₂ (HEen = *N*-(2-hydroxyethyl)-1,2-diaminoethane (**4**), [Ni(AEN)][B₅O₆(OH)₄]·H₂O (AEN = 1-(3-azapropyl)-2,4-dimethyl-1,5,8-triazaocta-2,4-dienato(1-)) (**5**), *trans*-[Ni(dach)₂(H₂O)₂][Ni(dach)₂][B₇O₉(OH)₅]₂·4H₂O (dach = 1,2-diaminocyclohexane (**6**), and the neutral species *trans*-[Ni(en)(H₂O)₂]{B₆O₇(OH)₆}]·H₂O (**7**) (en = 1,2-diaminoethane), and [Ni(dmen)(H₂O){B₆O₇(OH)₆}]·5H₂O (**8**). Compounds **1–8** were characterized by single-crystal XRD studies and by IR spectroscopy and **2, 4–7** were also characterized by thermal (TGA/DSC) methods and powder XDR studies. The solid-state structures of all compounds show extensive stabilizing H-bond interactions, important for their formation, and also display a range of gross structural features: **1** has an insular tetraborate(2-) anion, **2–5** have insular pentaborate(1-) anions, **6** has an insular heptaborate(2-) anion ('O⁺' isomer), whilst **7** and **8** have hexaborate(2-) anions directly coordinated to their Ni^(II) centers, as bidentate or tridentate ligands, respectively. The Ni^(II) centers are either octahedral (**1–4, 7, 8**) or square-planar (**5**), and compound **6** has both octahedral and square-planar metal geometries present within the structure as a double salt. Magnetic susceptibility measurements were undertaken on all compounds.

Keywords: borate anions; H-bonding; heptaborate(2-); hexaborate(2-); Nickel(II) complex; oxidoborate; pentaborate(1-); self-assembly; templated synthesis; tetraborate(2-); X-ray structures



Citation: Altahan, M.A.; Beckett, M.A.; Coles, S.J.; Horton, P.N. Oxidoborates Templated by Cationic Nickel(II) Complexes and Self-Assembled from B(OH)₃. *Inorganics* **2021**, *9*, 68. <https://doi.org/10.3390/inorganics9090068>

Academic Editors:
Jean-François Halet and
Gilles Alcaraz

Received: 19 August 2021
Accepted: 30 August 2021
Published: 31 August 2021

Publisher's Note: MDPI stays neutral with regard to jurisdictional claims in published maps and institutional affiliations.



Copyright: © 2021 by the authors. Licensee MDPI, Basel, Switzerland. This article is an open access article distributed under the terms and conditions of the Creative Commons Attribution (CC BY) license (<https://creativecommons.org/licenses/by/4.0/>).

1. Introduction

Synthetic borates (oxidoborates is the IUPAC recommended name for this class of compounds [1]) show great structural diversity and their structures complement the variety of structural motifs observed in borate minerals [2–5]. Borate minerals have large scale economic importance [6–8] (e.g., as vitreous, agriculture, fire retardant products) and some of these minerals, and their synthetic counterparts, have also found more specialist uses [9–18] (e.g., as fluorescent, optical SHG and wide band-gap semi-conductor materials).

Structurally, borates salts consist of metallic or non-metallic cationic centers and hydroxyoxidoborate units, with variable degrees of condensation, as either insular anions or as anionic 1-D chains, 2-D layers or 3-D networks [2–5]. Oxidoborate materials can be synthesized from aqueous solution or from solid-state or solvothermal methods and the latter non-aqueous methods often lead to the formation of the more highly condensed oxidoborate structures [5]. In aqueous solution, oxidoborate speciation is pH and boron-concentration dependent [19,20], and a dynamic combinatorial library (DCL) [21] of oxidoborate anions co-exist in rapidly attained aqueous equilibria.

Many oxidoborate anions have been successfully crystallized from aqueous solution using B(OH)₃ and an appropriate templating cation, e.g., triborate(1-), tetraborate(2-),

pentaborate(1-), hexaborate(2-), heptaborate(2-) (two isomers), heptaborate(3-), octaborate(2-) (two isomers), nonaborate(3-), tetradecaborate(4-), and pentadecaborate(3-) anions [5]. These salts are selectively templated from the solution by the cations present in self-assembly processes [22–24]. However, pentaborate(1-) salts often crystallize out of such solutions and this is particularly so if the cation is relatively small and has a charge of +1 [5]. This process primarily occurs since the $[B_5O_6(OH)_4]^-$ anion is ideally shaped to form giant H-bonded lattices through anion–anion interactions with ‘cavities’ large enough to be occupied by the small cations [25–28].

We are interested in expanding the structural diversity of isolated and coordinated oxidoborate chemistry and have developed a strategy of incorporating relatively highly charged ($>+1$) and/or cations, with the potential of forming multiple H-bond interactions, into the aqueous DCL of borate anions so that they can template and crystal engineer novel structures [29,30]. Using labile cationic transition-metal complexes [31] introduces a further DCL of potential cations into reaction medium and leads to the possibility of oxidoborate anions entering the primary coordination shell of the metal, as O-donor ligands.

With this in the forefront of our mind, we have recently investigated the reactions of labile complexes of $Zn^{(II)}$ [32–35] and $Cu^{(II)}$ [36–40] and have prepared novel species containing coordinated $[B_2O_3(OH)_2]^{2-}$ [39], $[B_5O_6(OH)_4]^-$ [37], $[B_6O_7(OH)_6]^{2-}$ [34–38], $[B_{12}O_{18}(OH)_6]^{6-}$ [32,35] and $[B_{20}O_{32}(OH)_8]^{12-}$ [39] ligands. $Ni^{(II)}$ complexes and their reactions with $B(OH)_3$ have received little attention to date and reported oxidoborate species are restricted to an unusual hexadentate tris(aminoethoxy)hexaborate(2-) anion complex, $[Ni\{(H_2NCH_2CH_2O)_3B_6O_7(OH)_3\}]$ [41], and a series of salts containing the insular pentaborate(1-) [42–47] or heptaborate(2-) [33,48] anions.

$Ni^{(II)}$ complexes have a d^8 electronic configuration and should also be relatively labile [31]. In this manuscript we report on the use coordination complexes of $Ni^{(II)}$ containing N-donor ligands NH_3 , en, dien, dmen, HEen, AEN, dach (see Figure 1 for ligand structures and abbreviations) to synthesize eight new oxidoborate compounds. Their single-crystal structures and their spectroscopic and physical properties are reported.

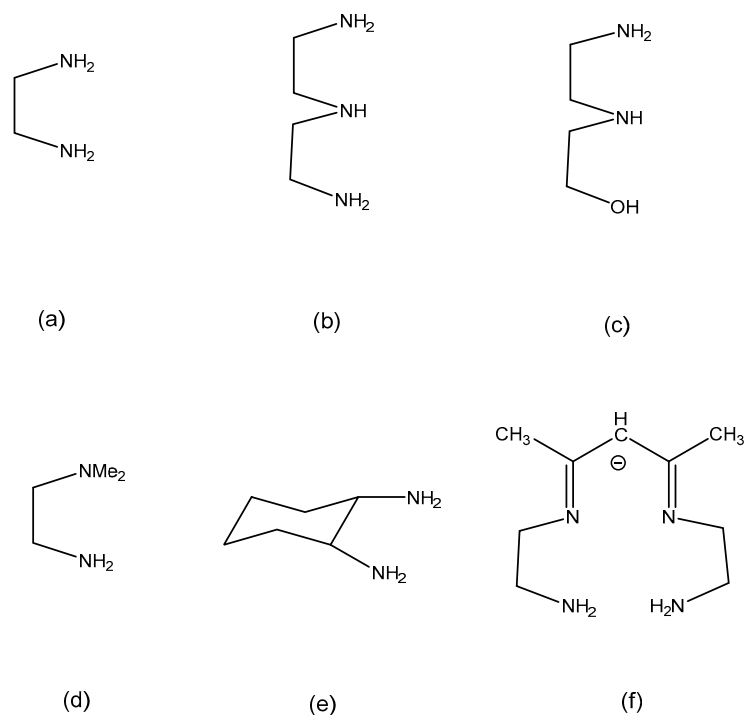
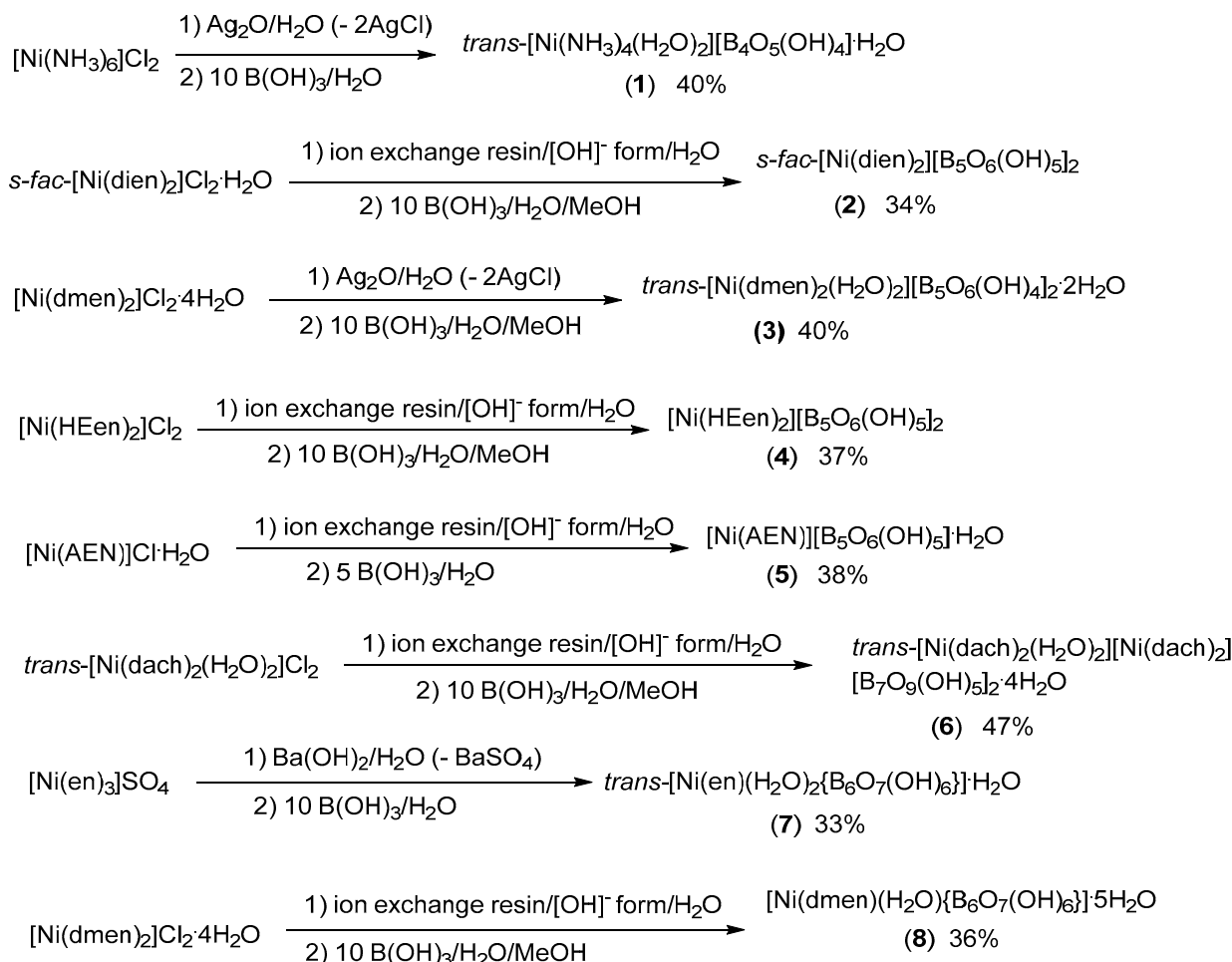


Figure 1. Drawings of the organic ligand structures found in compounds 1–8 with abbreviations as follows: (a) en, 1,2-diaminoethane, (b) dien, *N*-(2-aminoethyl)-1,2-ethanediamine, (c) HEen, *N*-(2-hydroxyethyl)-1,2-diaminoethane, (d) dmen, *N,N*-dimethyl-1,2-diaminoethane, (e) dach, 1,2-diaminocyclohexane, (f) AEN, 1-(3-azapropyl)-2,4-dimethyl-1,5,8-triazaocta-2,4-dienato(1-).

2. Results and Discussion

2.1. Synthesis and General Discussion

The Ni^(II) complex oxidoborates **1–8** were prepared in acceptable yields as a crystalline solids from the reaction of a Ni^(II) complex cation hydroxide salt with boric acid in a ratio of either 1:5 or 1:10 (Scheme 1). The Ni^(II) complex cation hydroxides were obtained in situ from the corresponding salts containing either chloride or sulfate anions. Anion exchange (from Cl[−]) was used for **2, 4, 5, 6,** and **8** and stoichiometric reactions with Ag₂O (from Cl[−]) was used for **1** and **3** and a stoichiometric reaction with Ba(OH)₂·8H₂O (from SO₄^{2−}) was used for **7**.



Scheme 1. Reagents and stoichiometry of reactants involved in self-assembly of Ni^(II) oxidoborates from cationic Ni^(II) complexes with B(OH)₃ in aqueous or methanolic aqueous solution.

The new compounds were identified by XRD single-crystal studies (Section 2.2), IR spectroscopic analysis and accompanied by thermal decomposition analysis (TGA and DSC) and powder XRD studies for **2, 4–7** (Section 2.3). Six of these eight compounds contain insular oxidoborate anions and two compounds contain coordinated hexaborate(2-) anions; the oxidoborate anions found in these new compounds are drawn out in Figure 2. The coordination geometry around the Ni^(II) centers are either octahedral (**1–4, 7, 8**) or square-planar (**5**) and compound **6** has both octahedral and square-planar metal geometries present within the structure as a double salt. The new Ni^(II) oxidoborate complexes are coloured with those with square-planar centres (**5** and **6**) are orange/red with the others having blueish hues. All compounds were stable in the solid state were insoluble in organic solvents and decomposed by aqueous solution (see ¹¹B NMR, Section 2.3). Since the products arise through self-assembly processes that we believe are associated with H-

bonded structure directing effects induced by the cations present [21–24], these interactions are discussed in detail in Section 2.2.2.

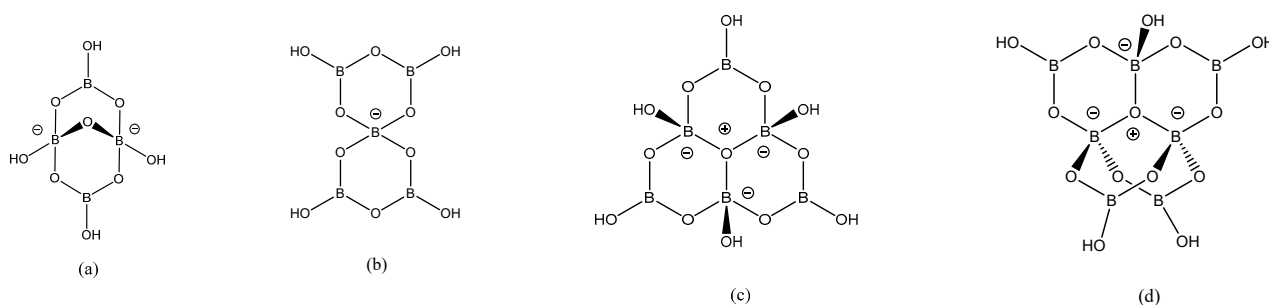


Figure 2. Drawings of the oxidoborate structures found in (a) **1**, (b) **2–5**, (c) **7, 8** and (d) **6**.

2.2. Crystallographic Studies on 1–8 and Their Solid-State H-Bonding Interactions

2.2.1. General Considerations for 1–6 and the Structures of 7 and 8

Selected crystallographic data for **1–8** can be found in Experimental Methods (Section 3) and full crystallographic details are available as Supplementary Materials. Compounds **1–6** are all anionic compounds containing discrete insular cationic Ni^(II) coordination complexes with *N*-donor or *O*-donor ligands, partnered with anionic oxidopolyborate anions. The cations in **2–6** are as found in their precursor complexes whilst **1** contains the partially aquated *trans*-[Ni(NH₃)₄(H₂O)₂]²⁺ cation. The cationic charges are neutralized by the insular oxidopolyborate anions [B₄O₅(OH)₄]²⁻, [B₅O₆(OH)₄]⁻, or [B₇O₉(OH)₅]²⁻ for **1**, **2–5** and **6**, respectively. Compounds **1**, **3**, **5** and **6** also contain one, two, one and four interstitial H₂O molecules per formula unit, respectively. The dien ligand in **2**, and the HEn ligand in **4** are both disordered over two positions. Compounds **7** and **8** are uncharged coordination compounds with [B₆O₇(OH)₆]²⁻ coordinated as *O*-donor ligands to octahedral Ni^(II) centres either as a bidentate or a tridentate ligand in **7** or **8**, respectively. Compounds **7** and **8** have one and five interstitial H₂O molecules, respectively, and are also partially aquated. There is some disorder of the interstitial H₂O molecules in both **7** and **8** and some additional disorder in the en ligand and the dmen ligands of **7** and **8**. Compound **6** is unusual and is best formulated as a double salt. It contains both octahedral *trans*-[Ni(dach)₂(H₂O)₂]²⁺ and square-planar [Ni(dach)₂]²⁺ cations partnered by two crystallographically equivalent [B₇O₉(OH)₅]²⁻ anions and four interstitial H₂O molecules. The dach ligands are also disordered in **6** but have chair conformations with their amino groups equatorial and with one dach ligand in each cation having *R,R* stereochemistry and the other *S,S*. Interestingly, two of these interstitial H₂O molecules (O22) in **6** are in ‘axial’ positions in the square-planar complex at 3.1517(13) Å (*T* = 0.61 [49]). In the octahedral complex, these two H₂O ligands (O21) are at 2.1422(15) Å (*T* = 0.98). A structurally related (but *d*⁹) Cu^(II) compound, prepared by an identical method [37], contains a square-planar (also with very long axial H₂O ‘bonds’, *T* = 0.70) and a Jahn–Teller distorted axially elongated octahedral complexes (*T* = 0.80). Structurally, the insular [B₇O₉(OH)₅]²⁻ dianion is previously known to adopt either a ‘chain’ or ‘O⁺’ isomeric forms [28,50–52] and the ‘O⁺’ isomer is present in **6**. The new Ni^(II) oxidoborate complex salts **1–6** all contain cations and anions that are known in other salts and the gross structures of the component ions, bond distances and internuclear angles for the component ions in **1–6** are as expected and need no further comment [5,53–55]. The uncharged complexes **7** and **8** are structurally novel although similar compounds have been observed in Co^(II), Cu^(II) and Zn^(II) oxidoborate chemistry [34–38,56–58]. Compounds **7** and **8** contain isolated species [35,37,38] rather than polymer 1-D coordination chains [34,36,38] and these two structures will be discussed in more detail below.

A drawing of the structure of *trans*-[Ni(en)(H₂O)₂{B₆O₇(OH)₆}]·H₂O (**7**), with selected crystallographic numbering, can be found in Figure 3. Compound **7** is a distorted neutral octahedral Ni^(II) complex with *trans* H₂O ligands (containing O21 and O22), a

disordered 1,2-diaminoethane ligand and a bidentate $[\text{B}_6\text{O}_7(\text{OH})_6]^{2-}$ ligand that is coordinated through two hydroxy groups (containing O8 and O9). A single disordered water of crystallization containing O31 (s.o.f. 0.47(2)) or O31B (s.o.f. 0.53(2)) is also shown. The O21-Ni1-O22 angle is $171.67(12)^\circ$ and the average Ni-(OH₂) distance is 2.089(3) Å. This average distance is slightly longer than the average oxidoborate O8/O9-Ni1 distance of 2.065(3) Å. The chelating en ligand significantly distorts the Ni^(II) centre where the Ni1-N1 and Ni1-N2 distances are 2.086(4) and 2.085(4) Å, respectively. The N1-Ni1-N2 angle is $82.80(16)^\circ$ and the oxidoborate/en ligand O8-Ni1-N2 and O9-Ni1-N1 angles are both significantly $<180^\circ$, whilst the O8-Ni1-O9 angle is $90.48(14)^\circ$. These Ni-N and Ni-(OH₂) bond lengths are within the expected ranges for Ni^(II) complexes [53–55] but this is the first example of a Ni-O bond length arising from an oxidoborate ligand and it is not significantly different from other N-O bond lengths. The B-O bond lengths and OBO and BOB angles of the hexaborate(2-) ligand are in accord with previously reported data for this ligand including three very long B-O bond lengths (1.498(6)–1.538(6) $^\circ$; av. 1.517(6) $^\circ$) to the three-coordinate O atom (O1) [28,29,48,51,52]. There is an intramolecular H-bond from an oxidoborate hydroxy group (containing O10) and the coordinated aqua ligand (containing O21), O10H10 \cdots O21, with a O10 \cdots O21 distance of 2.704(5) Å and a O10-H10-O21 angle of 144.9° (Figure 3). This H-bond is part of two R₁¹(8) rings [59] and both rings involve the Ni^(II) centre and two Ni-O coordinate bonds. There is a similar H-bond interaction in the only other known example of a bidentate hexaborate(2-) complex, $(\text{NH}_4)_2[\text{Zn}(\text{H}_2\text{O})_2(\text{B}_6\text{O}_7(\text{OH})_6)_2]$, but here, interestingly, the H-bond originates from the aqua ligand and the uncoordinated hydroxy site of the oxidoborate is the acceptor [35].

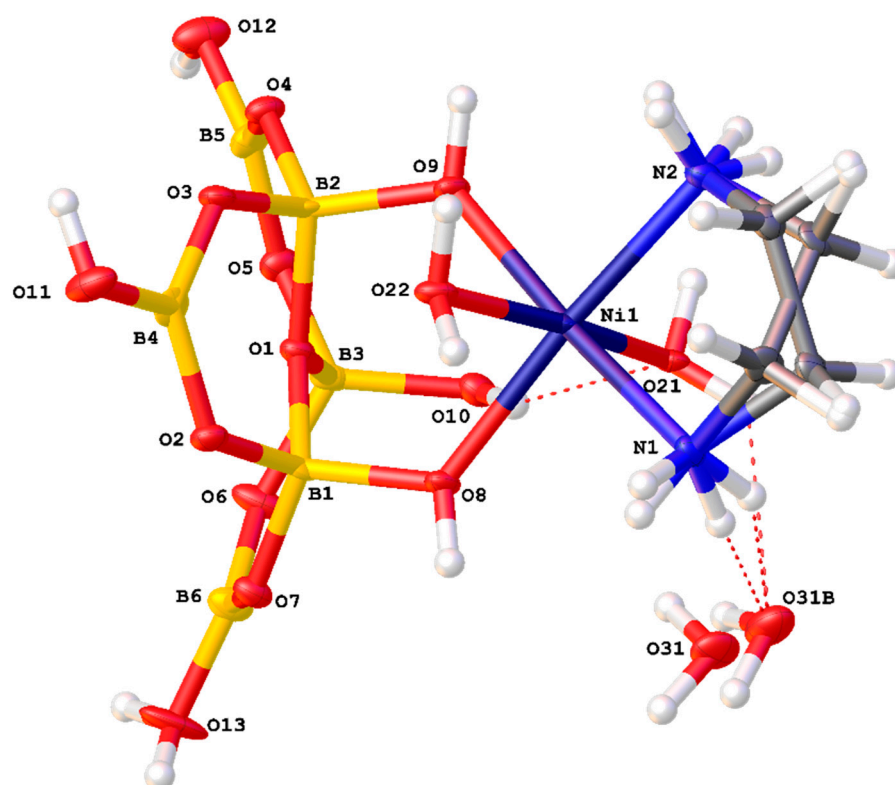


Figure 3. Drawing of structure *trans*-[Ni(en)(H₂O)₂{B₆O₇(OH)₆}]·H₂O (7), showing selected crystallographic numbering.

A drawing of the structure of [Ni(dmen)(H₂O){B₆O₇(OH)₆}]·5H₂O (8), with selected crystallographic numbering, is shown in Figure 4. Compound 8 is a distorted neutral octahedral Ni^(II) complex with disordered aqua ligand (containing O21) and dmen ligands (0.496(5) s.o.f shown) and a tridentate $[\text{B}_6\text{O}_7(\text{OH})_6]^{2-}$ ligand coordinated through three hydroxy groups (containing O11, O12 and O13). The five waters of crystallization contain

O31–O35. The Ni1–O21 distance for the aqua ligand (2.131(11) Å) is significantly longer than the Ni–O distances associated with the three hydroxy groups of the tridentate oxidoborate ligand (2.0415(17)–2.0978(17) Å; *av.* 2.078(2) Å) but this difference was not significant for **7**. The N1–Ni1–N2 angle associated with the chelating dmen ligand is 84.5(12)° and angles between the three O-donor atoms of the *fac*-hexaborate ligand range from 84.26(7)–90.66(6)°; *av.* 86.94(8)°. The aqua ligand with O21 is *trans* to oxidoborate O11 with an angle of 173.2(3)°, and the other *trans* angles are significantly <180.0°. The Ni1–N distances of 2.031(11) Å (N1) and 2.13(2) Å (N2) are significantly different but there is more steric demand at N2 as it is substituted by the two methyl groups. Overall, the bond lengths and angles associated with the Ni^(II) centre and those within the hexaborate(2-) ligand in **8** are in accord with comparable data for **7**.

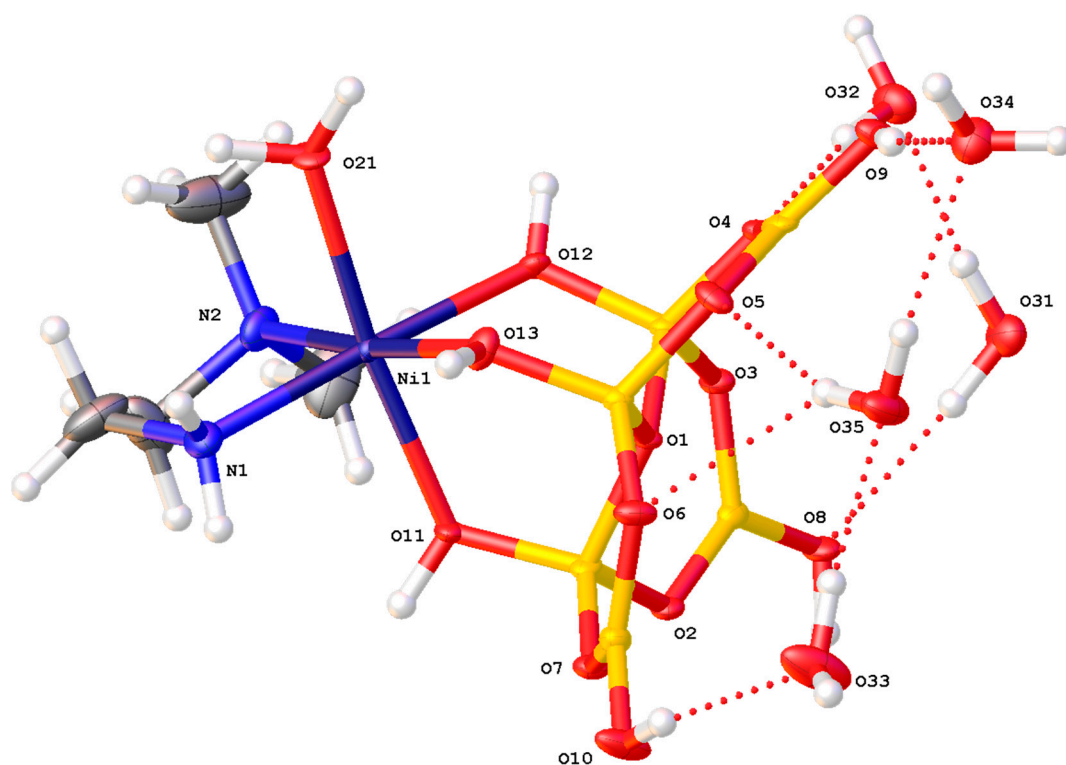


Figure 4. Drawing of structure of [Ni(dmen)(H₂O){B₆O₇(OH)₆]}·5H₂O (**8**), showing (selected) crystallographic numbering.

2.2.2. Solid-State H-Bonding Interactions in 1–8

Compounds **1–8** are self-assembled and crystallized from the various oxidoborate and the Ni^(II) amine complexes that are each in equilibrium in the reacting aqueous solution [19,20,31]. There is a strong preference for the oxidoborate anion to enter the primary coordination shell in related Cu^(II) and Zn^(II) chemistry with the formation of energetically favourable O-donor coordinate bonds [32,34–40,58]. Interestingly, Ni^(II) salts are described as labile, although in practice they are often considerably less labile than corresponding Cu^(II) and Zn^(II) complexes [31]. In accord with this, the Ni^(II) cations used in this study generally remain more or less intact in salts **1–6** after prolonged crystallization from aqueous solution, with formation of oxidoborate O-donor bonds only observed in compounds **7** and **8**. H-bond interactions also appear to be of paramount importance in driving this crystallization process and these interactions are described in detail for each compound in the following paragraphs.

A drawing of the components of the formula unit of **1**, showing important atomic numbering, is shown in Figure 5. The cations, anions and interstitial H₂O molecules have numerous H-bond donor and/or acceptor sites and all potential H-bond donor sites are used in the solid-state structure. The dotted red lines in Figure 5 illustrate H-

bond interactions which link cation to anion (O11H11 \cdots O6), cation to interstitial H₂O (N11H11 \cdots O21), and anion to interstitial H₂O (O6H6 \cdots O21) forming a R₂²(8) ring incorporating the Ni^(II) centre. These interactions as well as anion–anion interactions template the formation of the tetraborate salt. Full details of all H-bond interactions are available in the Supplementary Materials. Siveav and co-workers [46] have analysed H-bond interactions in tetraborate(2-) systems using the terminology of Zolotarev et al. [60] but we prefer the complimentary and more widely known Etter symbolism [59] in this manuscript. R₂²(8) interactions are very important at stabilizing hydroxyoxidopolyborate anions and three of the four boron based hydroxy centres are involved in such interactions: observed in R₂²(8) interactions are very important at stabilizing hydroxyoxidopolyborate anions and three of the four boron based hydroxy centres are involved in such interactions with O8-H8 \cdots O5' and O9'-H9' \cdots O3 paired in a R₂²(8) ring and O7-H7 \cdots O1' and O7'-H7' \cdots O1 forming a reciprocal pair in another R₂²(8) ring. The fourth boron based hydroxy group O6H6 is a donor to a H₂O molecule, O21 (Figure 5) forming an unusual R₃³(8) ring {Ni1-O11A-H11A \cdots O6-H6 \cdots O21 \cdots H11E-N11} and is also part of a larger R₄⁴(12) ring {O6-H6 \cdots O21-H21A \cdots O3'-B1'-O6'-H6' \cdots O21'-H21A' \cdots O3-B1-} (Figure 6). Since the cation is involved in templating the structure its H-bond interactions are very important and these include O11-H11A \cdots O6, O11-H11B \cdots O8, O12-H12A \cdots O4, O12-H12B \cdots O2, N14-H14A \cdots O8, N12-H12D \cdots O7 and N12-H12C \cdots O7 which originate from the aqua or ammine ligands. Further patterns are difficult to visualize although R₂²(8) {Ni1-N12-H12C \cdots O7-B2-O2 \cdots H12B-O12-} and a C₂²(10) {Ni1-O11-H11A \cdots O6-B1-O3-B3-O8 \cdots H14A'-N14'-} are discernable.

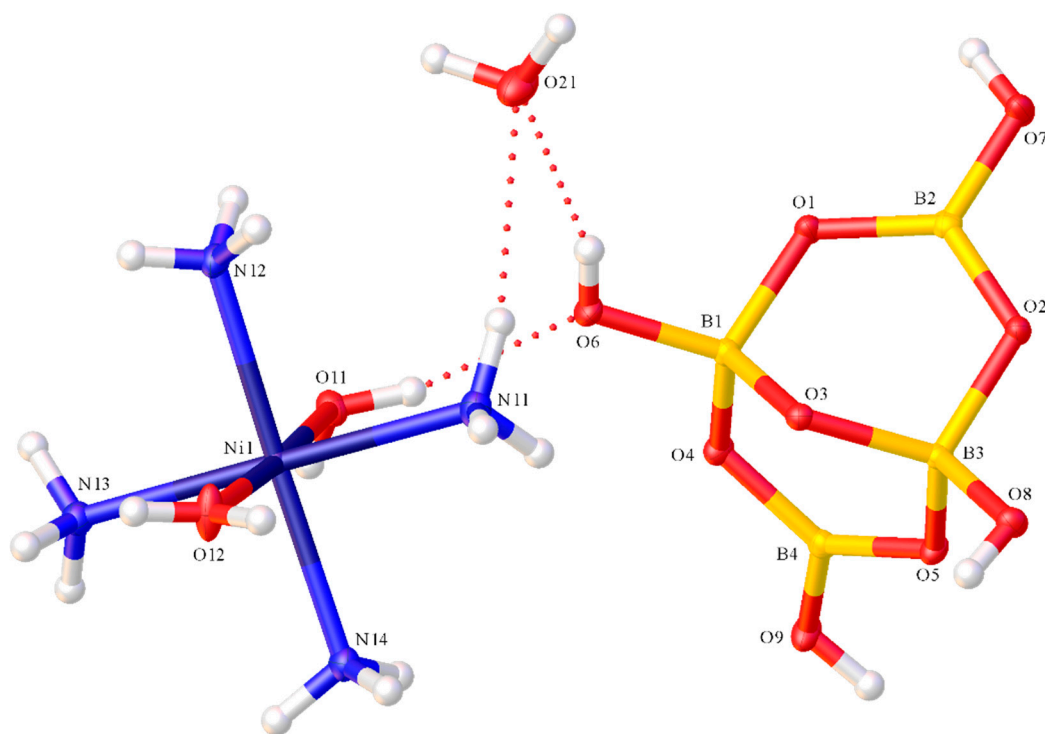


Figure 5. Drawing of structure of *trans*-[Ni(NH₃)₄(H₂O)₂][B₄O₅(OH)₄]·H₂O [Ni(dmen)(H₂O){B₆O₇(OH)₆}]·5H₂O (1), showing (selected) crystallographic numbering and the R₃³(8) ring system: {Ni1-O11A-H11A \cdots O6-H6 \cdots O21 \cdots H11E-N11}.

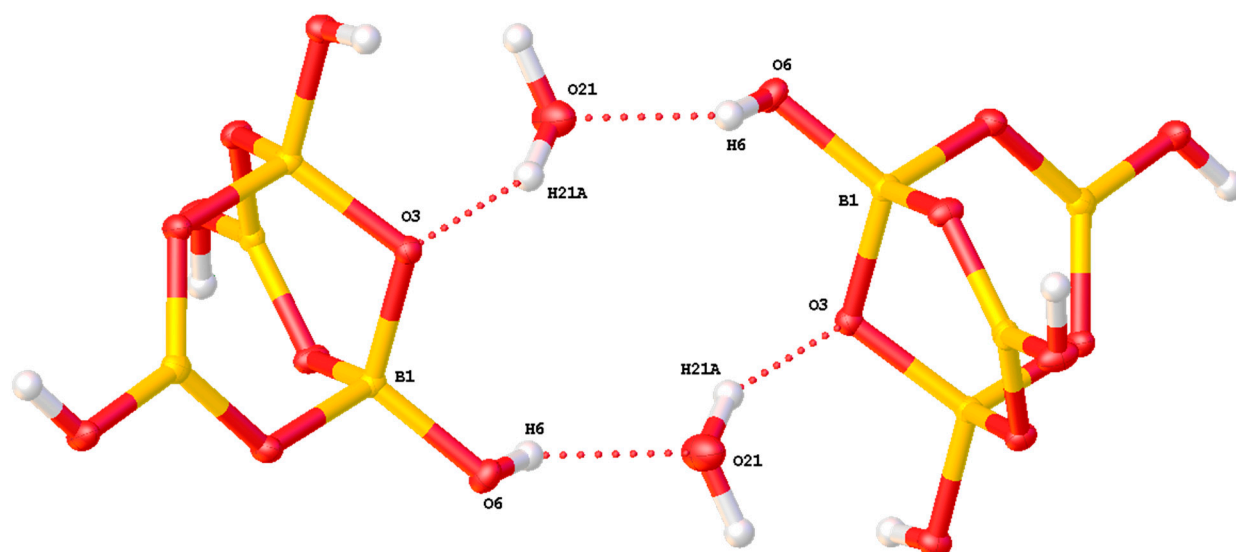


Figure 6. Drawing of the $R_4^4(12)$ ring, $\{O6-H6 \cdots O21-H21A \cdots O3'-B1'-O6'-H6' \cdots O21'-H21A' \cdots O3-B1-\}$, in *trans*- $[\text{Ni}(\text{NH}_3)_4(\text{H}_2\text{O})_2][\text{B}_4\text{O}_5(\text{OH})_4] \cdot \text{H}_2\text{O}$ (**1**).

Compounds **2–5** are all pentaborate(1-) salts and anion–anion H-bond interactions are well known to strongly influence their formation [5,25–28] since each pentaborate(1-) anion has four donor H-bond sites that are sterically arranged to form 3D H-bonded anionic giant structures, in which the cations occupy vacant ‘open-sites’ in the anionic lattice. The anion–anion interactions are conveniently described using a combination of ‘acceptor-sites nomenclature’, as defined by Schubert [26], and Etter terminology [59]. Compounds **2–4** have very similar anion–anion interactions and the four acceptor sites can be described as $\alpha, \alpha, \alpha, \beta$ with the α -site interactions reciprocal $R_2^2(8)$ and the β -interactions reciprocal $R_2^2(12)$; both types of interactions are common in pentaborate(1-) structures [5,27]. The anion interactions in **5** are different with three pentaborate(1-) acceptor sites (α, α, γ), all reciprocal $R_2^2(8)$, and an interstitial H_2O acceptor site. The cations in **2–5** are situated within the anionic lattices and have the potential to be H-bond donors (and acceptors) which can further stabilize the anionic lattices and help to template their self-assembly. Examples of such interactions, which involve novel ring systems that incorporate the Ni^{III} centres, ligands interstitial molecules and pentaborate(1-) anions, are $R_4^4(14)$ $\{\text{Ni1-N3B-H3B} \cdots \text{O10-O1OH} \cdots \text{O9-O9H} \cdots \text{O4-B1-O1-B2-O7} \cdots \text{H2B-N2B-\}$ (**2**) (includes three pentaborate(1-) anions), $R_2^2(8)$ $\{\text{Ni1-O11-H11B} \cdots \text{O7-B2-O2} \cdots \text{H12A-N12-\}$ (**3**) (one pentaborate(1-) anion), $R_2^2(8)$ $\{\text{Ni1-N11-H11D} \cdots \text{O11-B2-O7} \cdots \text{H11-O11-\}$ (**4**) (one pentaborate(1-) anion) and $R_2^2(8)$ $\{\text{Ni1-N11-H11D} \cdots \text{O1-B2-O7} \cdots \text{H11-O11-\}$ (**4**) (one pentaborate(1-) anion), and $R_4^4(16)$ $\{\text{Ni1-N1-H1C} \cdots \text{O5-B4-O4-B1-O3} \cdots \text{H1A-O11} \cdots \text{H7-O7-B2-O1} \cdots \text{H4A-N4-\}$ (**5**) (two pentaborate(1-) anions and one interstitial H_2O with O11). The $R_2^2(8)$ interaction for **3** is illustrated in Figure 7. Full details of all these interactions (and associated atomic numbering systems) are available in the Supplementary Materials.

Compound **6** is a heptaborate(2-) salt with numerous opportunities for interionic H-bonding interactions with the each anion possessing 14 potential acceptor sites and five donor sites and the two cations potentially having 20 donor sites and four acceptor sites; there are also four interstitial H_2O molecules. Potentially templating cation–anion interactions include the $R_2^2(8)$ $\{\text{Ni1-N12-H12A} \cdots \text{O10-B4-O3} \cdots \text{H11A-N11-\}$, the $R_3^3(8)$ $\{\text{Ni2-N12-H12D} \cdots \text{O23-H23B} \cdots \text{O11} \cdots \text{H11D-N11-\}$, and the $R_2^2(10)$ $\{\text{Ni1-O21-H21B} \cdots \text{O14-B1-O1-B2-O6} \cdots \text{H2B-N2-\}$. The familiar $R_2^2(8)$ anion–anion interaction is present in $\{\text{O12-H12} \cdots \text{O9'-B7'-O13'-H13'} \cdots \text{O7-B6-\}$ and the reciprocal $\{\text{O11-H11} \cdots \text{O5'-B5'-O11'-H11'} \cdots \text{O5-B5-\}$ and there is also a $R_2^2(12)$ interaction, $\{\text{O10-H10} \cdots \text{O8'-B2'-O2'-B4'-O10'-H10'} \cdots \text{O8-B2-O2-B4-\}$. The fifth heptaborate hydroxy group (containing O14) does not form a donor bond but O14 has a $R_2^2(10)$ acceptor interaction with a cation, as described above.

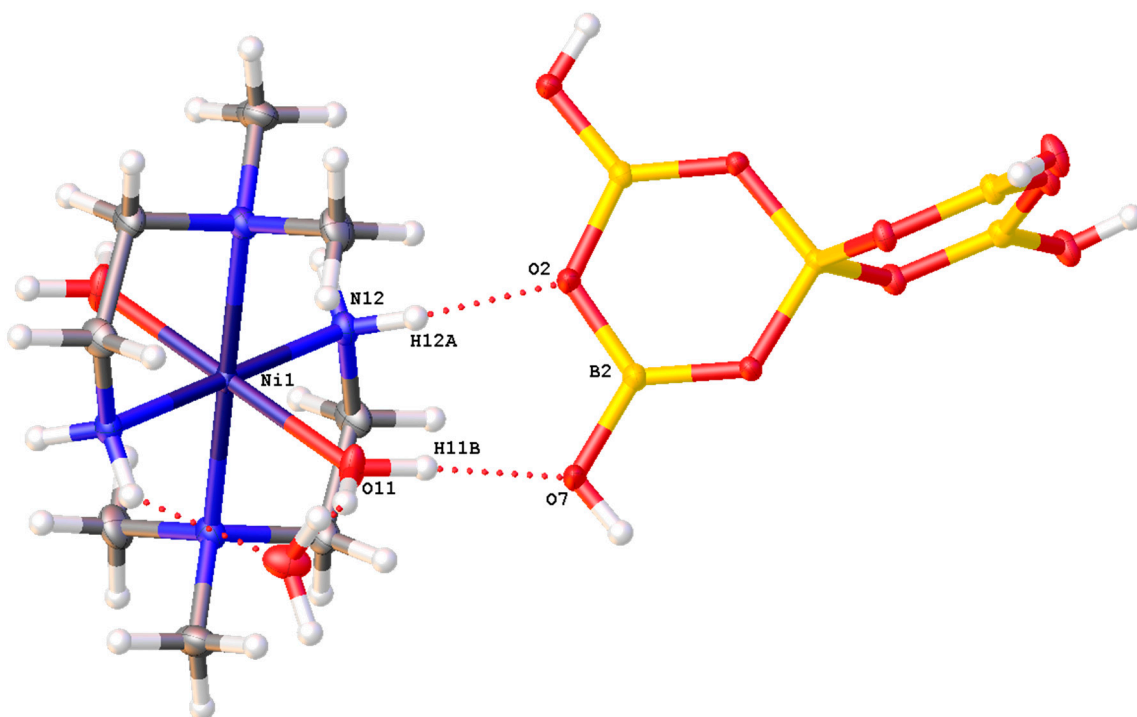


Figure 7. Drawing of the $R_2^2(8)$ {Ni1-O11-H11B...O7-B2-O2...H12A-N12-} interaction involving the Ni^(II) in *trans*-[Ni(dmen)₂(H₂O)₂] [B₅O₆(OH)₄]₂·2H₂O (**3**).

Intermolecular H-bonding, in addition to the intramolecular interaction found in **7** (Section 2.2.1) can be found in **7** and **8**. Such interactions for **7** include $R_2^2(6)$ {Ni1-O8-H8...O2...H1AA-N1-} and {Ni1-O9-H9...O3...H2BD-N2-}, $R_4^4(8)$ {O21-H21B...O10H10...O21'-H21B'...O10'-H10'...} and a reciprocal $R_2^2(12)$ {O12-H12...O6'-B3'-O5'-B5'-O12'-H12'...O6-B3-O5-B5-}. There are five interstitial H₂O's per Ni^(II) centre in **8** and their main roles are to act as 'spacers' [28] by forming H-bond bridges between neutral Ni^(II) oxidoborate complexes. Templating interactions occur when the oxidoborate ligand of one complex enters the second coordination sphere of another. This occurs in reciprocal oxidoborate ligand $R_2^2(12)$ interactions, {O11-H11...O10'-B6'-O7'-B1'-O11'-H11'...O10-B6-O7-B1-} and {O12-H12...O9'-B5'-O4'-B2'-O12'-H12'...O9-B5-O4-B2-}; these are that similar to one observed in **7** and in another heptaborate(2-) system [52]. A $R_2^2(8)$ {O8-H8...O2'-B4'-O8'-H8'...O2-B4-} interaction also links oxidoborate sections of neighbouring complexes.

2.3. Magnetic, Spectroscopic, Thermal and *p*-XRD Characterization of Compounds 1–8

Magnetic susceptibility measurements on **1–8** confirmed that all, excepting **5**, are paramagnetic with χ_m values ranging from 2500×10^{-6} to 3600×10^{-6} cm³·mol⁻¹ (μ_{eff} of 2.6–3.0 BM) corresponding to two unpaired electrons per formula unit. Compound **5** is diamagnetic ($\chi_m = -170 \times 10^{-6}$ cm³·mol⁻¹), and this value is in accord with the Ni^(II) centre being square-planar. The χ_m values of **1–4**, **7** and **8** are typical of octahedral Ni^(II) complexes [61] and have similar values to those obtained for the starting octahedral Ni^(II) complexes. Compound **6** is unusual in that it has a μ_{eff} corresponding to two unpaired electrons but there are *two* Ni^(II) centres in the formula unit; the XRD study confirmed that one Ni^(II) centre is square planar and the other is octahedral.

Compound **5**, in D₂O solvent, gave ¹H and ¹³C NMR signals for the AEN ligand at similar intensities and chemical shifts to those obtained for [Ni(AEN)]Cl·H₂O and other reported data [62]. ¹H and ¹³C NMR signals for the organic ligands (in D₂O) were not observable for the other Ni^(II) oxidoborates despite their apparent solubility, due to their paramagnetic properties. Despite the possible lability of the organic ligands the complexes the organic ligands are not sufficiently labile to be remote from the Ni^(II) centres during the lifetime of the NMR experiment. ¹¹B NMR spectra for *all* D₂O solutions arising from

the Ni^(II) oxidoborates were observed and a probable explanation for this being two-fold: (i) compounds with insular oxidoborate anions (1–6) are not coordinated to the Ni^(II) centres and hence are not in close proximity and unaffected by the paramagnetic centres, and (ii) the coordinated hexaborate(2-) ligands are significantly more labile than the *N*-donor ligands in 7 and 8. The ¹¹B spectra were not particularly characteristic of the specific oxidopolyborate anions in 1–8 since it is known that dissolution of oxidopolyborate anions in aqueous solution yields solutions containing equilibrium mixtures of various oxidopolyborate anions whose concentrations are pH or boron concentration dependent [19,20]. However, pentaborate(1-) salts often afford spectra in a characteristic pattern with three signals at ca. +17, +13 and +1 ppm which have been assigned to B(OH)₃/[B(OH)₄][−], [B₃O₃(OH)₄][−] and [B₅O₆(OH)₄][−] species [5,27,28]; compounds 2–4 all showed this characteristic pattern. Dilute solutions often give just one signal, assigned to B(OH)₃/[B(OH)₄][−], at a chemical shift which is variable [19] but can be calculated assuming fast exchange of B(OH)₃/[B(OH)₄][−] according to their relative proportions present in the oxidopolyborate anion originally present [27]. Unsurprisingly, therefore, compounds 1 and 5–8 all gave single signals at +11.1, +16.3, +15.8, +17.7 and +15.8 ppm respectively. The observed chemical shifts for the tetraborate(2-) (1) and the pentaborate(-) (5) salts are as would be expected from this calculation (+11.0 and +16.1, respectively) but chemical shifts for the hexaborate(2-) (7 and 8) and the heptaborate(2-) (6) salts are ca. 2 ppm more downfield than expected (13.8 and 14.6 ppm calc., respectively), indicating that more B(OH)₃ might be present than expected. Similar behaviour has been observed before for hexaborate [34–38] and heptaborate [33] complexes.

Vibration spectroscopy is often used to help characterize oxidopolyborate species since strong, and often diagnostic, B-O stretches can be observed by IR spectroscopy between 1600 and 600 cm^{−1} [63]. In particular, diagnostic bands have been reported for pentaborate(1-) [5,27,28,64], hexaborate (2-) [35,37,63], and heptaborate(2-) [28,33,52] anions. Compounds 1–8 all displayed such diagnostic bands with the diagnostic band for the pentaborate(1-) anion (ca. 1925 cm^{−1}) clearly present in 1–5. Likewise, the diagnostic bands for hexaborate(2-) anion (ca. 960 and 810 cm^{−1}) and the heptaborate(2-) anion (ca. 860 cm^{−1}) were observed in IR spectra of 6 and 7, and 8, respectively.

Selected Ni^(II) oxidoborates (2, 4–7) were thermally decomposed air and insights into these decompositions were obtained through TGA/DSC studies. The Ni^(II) oxidoborates all yielded green glassy residues by 700 °C with masses consistent with anhydrous Ni^(II) oxidoborates being produced with Ni:B stoichiometries in the elemental ratios of their precursors. Thus, the pentaborates 2 and 4 were decomposed to NiB₁₀O₁₆ whilst 5 gave Ni₂B₁₀O₁₇, the heptaborate (6) gave Ni₂B₁₄O₂₃ and the hexaborate (7) yielded NiB₆O₁₀. These decomposition reactions are generally two-step processes with the first steps being a lower temperature (<280 °C) endothermic dehydration (loss of interstitial H₂O and condensation reactions of the hydrated oxidoborates) followed by higher temperature (280–700 °C) exothermic oxidations of the organic ligands. Details for individual compounds (2, 4–7) are given in the experimental section. This type of decomposition behaviour has been observed previously for other hydrated Ni^(II) oxidoborates [33,42–48] and more generally applies to the thermolysis of many hydrated transition-metal oxidopolyborates [30,33,35,37]. Powder XRD data were also obtained for this selection of Ni^(II) oxidoborates (*viz.* 2, 4–7). The data obtained were good matches with data calculated from the single-crystal XRD data indicating that these samples were crystalline and homogeneous.

3. Experimental Methods

3.1. General

The Ni^(II) complexes *s-fac*-[Ni(dien)₂]Cl₂·H₂O [65] [Ni(dmen)₂]Cl₂·4H₂O [66], [Ni(HEen)₂]Cl₂ [67], [Ni(AEN)]Cl₂·H₂O [62], *trans*-[Ni(dach)₂(H₂O)₂]Cl₂ [68] were prepared by modified literature procedures. FTIR spectra were obtained as KBr pellets on a Perkin–Elmer 100FTIR spectrometer (Perkin–Elmer, Seer Green, UK). ¹¹B NMR spectra were obtained on a Bruker Avance-400 spectrometer (Bruker, Coventry, UK) on samples

dissolved in D₂O at 128 MHz. TGA and DSC were performed on an SDT Q600 instrument (TA Instruments, New Castle DE, USA) using Al₂O₃ crucibles with a ramp rate of 10 °C per minute (RT to 1000 °C in air). X-ray crystallography was performed at the EPSRC national crystallography service centre at Southampton University. Magnetic susceptibility measurements were performed on a Johnson–Matthey magnetic susceptibility balance. (Johnson–Matthey, UK). CHN analyses were obtained from OEA Laboratories (Callingham, Cornwall).

3.2. X-ray Crystallography

Crystallographic data for 1–8 are given in the experimental section. The crystallographic data collection of compounds were performed on a Rigaku FR-E+ diffractometer (1, 3–8) equipped with an AFC12 goniometer, an HG Saturn 724+ detector and either HF varimax confocal mirrors (1, 3, 4, 6–8) or VHF varimax confocal mirrors (5). Data for 2 were obtained on DLS synchronous beamtime 119 equipped with a crystallographic goniometer and a Rigaku HG Saturn 724 detector. Data for all compounds were obtained at 100(2)K. Cell determinations and data collections were carried out using either CrysAlisPro [69] (1) or CrystalClear [70] (2–8). Data reduction, cell refinement and absorption correction were carried out using either CrysAlisPro [69] (1–3, 5–8) or CrystalClear [70] (4). Using Olex2 [71] the structures were solved using SHELXT [72] and models or refined with SHELXL [73]. Structure refinement details are given in the Supplementary Material. CCDC 2101911–2101918 (1–8 respectively), contains the supplementary crystallographic data for this paper. These data can be obtained free of charge via <http://www.ccdc.cam.ac.uk/conts/retrieving.html> (or from CCDC, 12 Union Road, Cambridge, CB2 1EZ. Fax: +44 1223 336033; E-mail: deposit@ccdc.cam.ac.uk)

3.3. Preparation of *Trans*-[Ni(NH₃)₄(H₂O)₂][B₄O₅(OH)₄]·H₂O (1)

NiCl₂·6H₂O (1.00 g, 4.0 mmol) dissolved in ethanol (25 mL) and gave a clear green solution. Aqueous NH₃ solution (2.2 mL, 25%, 24 mmol) was added dropwise to the green solution with stirring and then was left to stir for a further 5 min to give a dark blue solution. Ag₂O (0.926 g, 4 mmol) was rapidly added and stirred at room temperature for 5 min and the precipitate which had formed (AgCl) was removed by filtration. B(OH)₃ (1.23 g, 20 mmol) was added to the dark blue filtrate and left to stir for a further 10 min. The reaction mixture was filtered into vials and left to allow for slow evaporation of the solvent. After 2 weeks a light blue solid (1) had formed in the bottom of a vial and this was collected by filtration. (0.6 g, 40%). M.p. ≥ 300 °C. $\chi_m = 2500 \times 10^{-6} \text{ cm}^3 \cdot \text{mol}^{-1}$. H₂₂B₄N₄NiO₁₂. Anal. Calc.: H = 6.0%, N = 15.1%. Found: H = 5.7%, N = 15.3. ¹¹B/ppm: 11.1. IR (KBr/cm⁻¹): 3375(s), 3245(s), 1634(m), 1450(s), 1402(s), 1345(s), 1230(m), 1152(m), 1059(m), 1002(s), 936(m), 828(m). sc-XRD crystal data: $M_r = 372.16$, monoclinic, $P2_1/c$ (No. 14), $a = 8.27730(10) \text{ \AA}$, $b = 20.5277(3) \text{ \AA}$, $c = 8.01330(10) \text{ \AA}$, $\beta = 91.2830(10)^\circ$, $\alpha = \gamma = 90^\circ$, $V = 1361.23(3) \text{ \AA}^3$, $T = 100(2) \text{ K}$, $Z = 4$, $Z' = 1$, $\mu(\text{MoK}\alpha) = 1.492 \text{ mm}^{-1}$, 15,477 reflections measured, 3128 unique ($R_{int} = 0.0329$) which were used in all calculations. The final wR_2 was 0.0528 (all data) and R_1 was 0.0216 ($I > 2\sigma(I)$).

3.4. Preparation of *s-fac*-[Ni(dien)₂][B₅O₆(OH)₄]₂ (2)

s-fac-[Ni(dien)₂]Cl₂·H₂O (1.05 g, 3.0 mmol) was dissolved in H₂O (10 mL) and added to a suspension of excess DOWEX[®] monosphere 550A OH⁻ activated anion exchange resin (Dupont, Wilmington, DE, USA) (40 g) in H₂O (40 mL). The mixture was left to stir for 30 h at RT and then filtered to remove the resin. The filtrate, containing *s-fac*-[Ni(dien)₂](OH)₂, was reduced in volume to 15 mL and MeOH (15 mL) was added. B(OH)₃ (1.83 g, 29.7 mmol) was added to the H₂O/MeOH solution which was then gently warmed with stirring for 3 h. The solution was concentrated to 5 mL under reduced pressure and the concentrated solution was left for a few days for crystallization. Purple crystals of 2 were carefully recovered by filtration and dried in air (0.70 g, 34%). M.p. = 287–289 °C (dec.). $\chi_m = 3516 \times 10^{-6} \text{ cm}^3 \text{ mol}^{-1}$. C₈H₃₄B₁₀N₆NiO₂₀. Anal. Calc.: C = 13.7%, H = 4.9%,

N = 12.0%. Found: C = 14.0%, H = 5.4%, N = 12.1%. ^{11}B /ppm: 1.5 (1%), 13.3 (13%), 17.4 (86%). IR (KBr/cm $^{-1}$): 3362(s), 3333(s), 3297(s), 3263(s), 1412(s), 1330(s), 1303(s), 1135(m), 1059(m), 1042(m), 1028(m), 964(m), 931(m), 915(s), 774(s), 772(m), 707(s). TGA: 100–200 °C, condensation of polyborate which loss of four H $_2$ O 14.9% (10.2% calc.); 200–650 °C, oxidation of organic content 40.3% (39.7% calc.); residual NiB $_8$ O $_{13}$ 59.7% (60.3% calc.). p-XRD d-spacing/Å (% rel. int.): 6.22 (24), 5.88 (100), 5.57 (94), 4.27 (15), 3.79 (19), 3.71 (28), 2.94 (17). sc-XRD crystal data: M_r = 701.22, triclinic, P -1 (No. 2), a = 8.5763(5) Å, b = 9.2902(6) Å, c = 9.3493(6) Å, α = 78.098(5)°, β = 89.108(5)°, γ = 89.110(5)°, V = 728.75(8) Å 3 , T = 100(2) K, Z = 1, Z' = 0.5, μ (Synchrotron $_{0.6889\text{\AA}}$) = 0.702 mm $^{-1}$, 6342 reflections measured, 3152 unique (R_{int} = 0.0476) which were used in all calculations. The final wR_2 was 0.2109 (all data) and R_1 was 0.0767 ($I > 2\sigma(I)$).

3.5. Preparation of Trans-[Ni(dmen) $_2$ (H $_2$ O) $_2$][B $_5$ O $_6$ (OH) $_4$] $_2$ ·2H $_2$ O (3)

[Ni(dmen) $_2$]Cl $_2$ ·4H $_2$ O (0.97 g, 3.0 mmol), and Ag $_2$ O (0.75 g, 3.2 mmol) were rapidly stirred in H $_2$ O (30 mL) at room temperature for 40 min and the precipitate which had formed (AgCl) was removed by filtration. B(OH) $_3$ (1.85 g, 30 mmol) was added to the dark blue filtrate and left to stir for a further 40 min. The reaction mixture was filtered into vials and then left to allow for slow evaporation of solvent. After 3 weeks a light blue solid (3) had formed in the bottom of a vial and this was collected by filtration. (0.9 g, 40%). M.p. \geq 300 °C. χ_m = 3600 \times 10 $^{-6}$ cm 3 ·mol $^{-1}$. C $_8$ H $_{40}$ B $_{10}$ N $_4$ NiO $_{24}$. Anal. Calc.: C = 12.9%, H = 5.4%, N = 7.5%. Found: C = 13.0%, H = 5.5%, N = 7.5%. ^{11}B /ppm 16.6 (85%), 13.9 (14%), 1.2 (1%). IR (KBr/cm $^{-1}$): 3510 (m), 3348(s), 3285(s), 1608(m), 1415(s), 1310(s), 1129(m), 1043(m), 1015(m), 920(s), 780(s), 707(m), 486(m). sc-XRD crystal data: M_r = 743.25, triclinic, P -1 (No. 2), a = 8.6570(3) Å, b = 9.7443(3) Å, c = 10.2101(3) Å, α = 107.087(3)°, β = 102.747(3)°, γ = 95.002(3)°, V = 792.23(5) Å 3 , T = 100(2) K, Z = 1, Z' = 0.5, μ (MoK $_{\alpha}$) = 0.708 mm $^{-1}$, 12,978 reflections measured, 3628 unique (R_{int} = 0.0163) which were used in all calculations. The final wR_2 was 0.0731 (all data) and R_1 was 0.0270 ($I > 2\sigma(I)$).

3.6. Preparation of [Ni(HEen) $_2$][B $_5$ O $_6$ (OH) $_4$] $_2$ (4)

The preparation of [Ni(HEen) $_2$](OH) $_2$ was carried out as described previously for 2 from [Ni(HEen) $_2$]Cl $_2$ (1.00 g, 2.95 mmol) and Dowex (40 g). B(OH) $_3$ (1.83 g, 29.6 mmol) was added with stirring. The reaction mixture was stirred for a further 2 h at room temperature. The solvent was then evaporated to 5 mL using a rotary evaporator, then the resulting solution was left for 10 d in several NMR tubes for crystallization to yield purple crystals of 4 (0.76 g, 37%). M.p. = 288–289 °C (dec.). χ_m = 3430 \times 10 $^{-6}$ cm 3 mol $^{-1}$ C $_8$ H $_{32}$ B $_{10}$ N $_4$ NiO $_{22}$. Anal. Calc.: C = 13.7%, H = 4.6%, N = 8.0%. Found: C = 13.7%, H = 4.7%, N = 8.0%. ^{11}B /ppm: 1.2 (3%), 13.4 (23%), 18.0 (74%). IR (KBr/cm $^{-1}$): 3375(s), 3288(s), 3322(s), 1410(s), 1321(s), 1196(m), 1141(s), 1022(s), 919(s), 774(s), 706(s). TGA: 230–290 °C, condensation of polyborate which loss of four H $_2$ O 10.3% (10.2% calc.); 290–700 °C, oxidation of organic content 37.9% (39.9% calc.); residual NiB $_{10}$ O $_{16}$ 62.1% (60.1 calc.). p-XRD d-spacing/Å (% rel. int.): 6.18 (40), 5.88 (75), 5.50 (100), 3.94 (26), 3.78 (38), 3.66 (25). sc-XRD crystal data: M_r = 703.18, Monoclinic, $P2_1/c$, a = 8.3891(2) Å, b = 11.6666(3) Å, c = 14.3092(4) Å, α = γ = 90°, β = 90.035(2)°, V = 1400.47(6) Å 3 , T = 100(2) K, Z = 2, Z' = 0.5, μ (MoK $_{\alpha}$) = 0.791 mm $^{-1}$, 6239 reflections measured, 6239 unique (R_{int} = 0) which were used in all calculations. The final wR_2 was 0.1124 (all data) and R_1 was 0.0499 ($I > 2\sigma(I)$).

3.7. Preparation of [Ni(AEN)][B $_5$ O $_6$ (OH) $_4$] $_2$ ·H $_2$ O (5)

The preparation of [Ni(AEN)](OH) was carried out as described previously for 2 from [Ni(AEN)]Cl·H $_2$ O (2.10 g, 7.0 mmol) and Dowex (25 g). B(OH) $_3$ (2.22 g, 36 mmol) was added to the aqueous solution which was gently warmed with stirring for 3 h, and then its volume was reduced to 5 mL under reduced pressure. The solution was then distributed in several NMR tubes for crystallization and left for 10 days to yield dark red crystals of 5 (1.30 g, 38%). M.p. = 279–280 °C (dec.). χ_m = -170×10^{-6} cm 3 mol $^{-1}$. C $_9$ H $_{25}$ B $_5$ N $_4$ NiO $_{11}$. Anal. Calc.: C = 22.6%, H = 5.3%, N = 11.7%. Found: C = 22.7%, H = 5.4%, N = 11.7%. ^1H /ppm: 2.0 (s,

6H, CH₃), 2.5 (t, 4H, *J* = 6 Hz, CH₂ of en), 3.2 (t, 4H, *J* = 6 Hz, CH₂ of en), 4.8 (s, 11H, NH₂, H₂O, OH, CH). ¹³C/ppm: 19.9, 43.0, 53.6, 160.5. ¹¹B/ppm: 16.3. IR (KBr/cm⁻¹): 3377(s), 3326(s), 3288(s), 3246(s), 3169(s), 1615(m), 1566(m), 1536(m), 1476(s), 1442(s), 1416(s), 1393(s), 1333(s), 1295(s), 1129(m), 1094(s), 1072(m), 1019(m), 924(s), 778(m). TGA: 100–180 °C, loss of one interstitial H₂O 2.5% (3.7% calc.); 180–280 °C, condensation of polyborate which loss of two further H₂O 10.0% (11.3% calc.); 280–700 °C, oxidation of organic content 46.1% (48.0% calc.); residual Ni₂B₁₀O₁₇ 53.9% (52.0% calc.). p-XRD d-spacing/Å (% rel. int.): 5.65 (69), 5.38 (100), 4.14 (46), 3.89 (33), 3.81 (53), 3.65 (58), 2.03 (41), 1.43 (33). sc-XRD crystal data: *M_r* = 478.09, Triclinic, *P*-1, *a* = 8.5386(2) Å, *b* = 11.3328(3) Å, *c* = 11.8717(3) Å, *α* = 115.914(3)°, *β* = 101.626(2)°, *γ* = 99.670(2)°, *V* = 968.39(5) Å³, *T* = 100(2) K, *Z* = 2, *Z'* = 1, *μ*(MoK_α) = 1.065 mm⁻¹, 16,639 reflections measured, 4433 unique (*R*_{int} = 0.0216) which were used in all calculations. The final *wR*₂ was 0.0765 (all data) and *R*₁ was 0.0278 (*I* > 2σ(*I*)).

3.8. Preparation of Trans-[Ni(dach)₂(H₂O)₂][Ni(dach)₂][B₇O₉(OH)₅]₂·4H₂O (6)

The preparation of [Ni(dach)₂(H₂O)₂](OH)₂ was carried out as previously described for **2** from *trans*-[Ni(dach)₂(H₂O)₂]Cl₂ (1.00 g, 2.53 mmol) and Dowex (40 g). B(OH)₃ (1.56 g, 25.2 mmol) was added to the solution which was then gently warmed with stirring for 3 h. The solution volume was reduced to 5 mL under reduced pressure. The product (**6**) was isolated by filtration, and then allowed to dry in an oven at 40 °C for 3 h to afford orange prismatic crystals (0.78 g, 47%). M.p. = 270–272 °C (dec.). *χ*_m = 3030 × 10⁻⁶ cm³ mol⁻¹. C₂₄H₇₈B₁₄N₈Ni₂O₃₄. Anal. Calc.: C = 22.3%, H = 6.1%, N = 8.7%. Found: C = 21.8%, H = 6.3%, N = 8.4%. ¹¹B/ppm: 15.8. IR (KBr/cm⁻¹): 3663(s), 3271(s), 2929(m), 2863(m), 1468(m), 1453(s), 1350(s), 1180(s), 1125(m), 1066(s), 986(w), 854(m), 807(m). TGA: 100–190 °C, loss of four interstitial and two coordinated H₂O 7.5% (8.4% calc.); 190–270 °C, condensation of polyborate which loss of five further H₂O 15.0% (15.3% calc.); 270–720 °C, oxidation of organic content 48.2% (50.7% calc.); residual Ni₂B₁₄O₂₃ 51.8% (49.3% calc.). p-XRD d-spacing/Å (% rel. int.): 10.67 (100), 9.81 (89), 6.25 (58), 5.35 (70), 4.26 (48), 3.74 (55), 2.03(59). sc-XRD crystal data: *M_r* = 645.85, Monoclinic, *C*2/*c*, *a* = 22.3539(4) Å, *b* = 11.0192(2) Å, *c* = 22.8834(4) Å, *α* = *γ* = 90°, *β* = 107.630(2)°, *V* = 5371.94(18) Å³, *T* = 100(2) K, *Z* = 8, *Z'* = 1, *μ*(MoK_α) = 0.806 mm⁻¹, 33628 reflections measured, 6154 unique (*R*_{int} = 0.0281) which were used in all calculations. The final *wR*₂ was 0.1087 (all data) and *R*₁ was 0.0384 (*I* > 2σ(*I*)).

3.9. Preparation of Trans-[Ni(en)(H₂O)₂][B₆O₇(OH)₆]₂·H₂O (7)

An aqueous solution of en (2.30 g, 70%, 26.79 mmol) was added to an aqueous solution (10 mL) of NiSO₄·6H₂O (2.12 g, 8.06 mmol). The reaction mixture was stirred for 5 min, and then an aqueous solution (10 mL) of Ba(OH)₂·8H₂O (2.54 g, 8.06 mmol) was added. The reaction mixture was stirred for 30 min and then filtered to remove the BaSO₄. A solution of B(OH)₃ (4.98 g, 80.6 mmol) in H₂O (10 mL) was added to the filtrate with stirring. The reaction mixture was stirred at room temperature for 2 h. The solution was then distributed in several vials and left for 10 d to yield faint blue crystals of **7** (1.20 g, 33%). M.p. = 245–247 °C (dec.). *χ*_m = 2588 × 10⁻⁶ cm³ mol⁻¹. C₂H₂₀B₆N₂NiO₁₆. Anal. Calc.: C = 5.3%, H = 4.5%, N = 6.2%. found: C = 5.4%, H = 4.5%, N = 6.2%. ¹¹B/ppm: 17.7. IR (KBr/cm⁻¹): 3400(s), 3350(s), 2924(w), 1420(m), 1380(s), 1360(s), 1133(s), 1095(s), 1044(s), 955(m), 908(m), 809(s). TGA: 100–180 °C, loss of one interstitial H₂O and two coordinated water molecules 0.8% (12% calc.); 180–280 °C, condensation of polyborate which loss of three further H₂O 24.3% (23.9% calc.); 280–700 °C, oxidation of organic content 38.6% (37.2% calc.); residual NiB₆O₁₀ 61.4% (62.8% calc.). p-XRD d-spacing/Å (% rel. int.): 9.78 (100), 8.26 (24), 6.77 (53), 4.88 (48), 3.99 (34), 3.38 (30), 2.74 (47). sc-XRD crystal data: *M_r* = 451.77, triclinic, *P*-1 (No. 2), *a* = 8.5116(7) Å, *b* = 9.7946(5) Å, *c* = 9.8073(8) Å, *α* = 89.873(5)°, *β* = 82.901(7)°, *γ* = 74.372(6)°, *V* = 780.94(10) Å³, *T* = 100(2) K, *Z* = 2, *Z'* = 1, *μ*(MoK_α) = 1.333 mm⁻¹, 5883 reflections measured, 5883 unique (*R*_{int} = 0) which were used in all calculations. The final *wR*₂ was 0.1902 (all data) and *R*₁ was 0.0682 (*I* > 2σ(*I*)).

3.10. Preparation of $[\text{Ni}(\text{dmen})(\text{H}_2\text{O})\{\text{B}_6\text{O}_7(\text{OH})_6\}]\cdot 5\text{H}_2\text{O}$ (8)

The preparation of $[\text{Ni}(\text{dmen})_2](\text{OH})_2$ was carried out as described for 2 from $[\text{Ni}(\text{dmen})_2]\text{Cl}_2\cdot 4\text{H}_2\text{O}$ (1.00 g, 2.6 mmol) and Dowex (30 g). $\text{B}(\text{OH})_3$ (1.57 g, 25 mmol) was added to the filtrate and left to stir for 30 min. The turquoise solution was filtered into vials and left to allow for slow evaporation of the solvents. After 2 weeks, a blue-green solid (8) had formed in the bottom of a vial and this was collected by filtration. Yield: (0.5 g, 36%). M.p. ≥ 300 °C. $\chi_m = 3050 \times 10^{-6} \text{ cm}^3 \text{ mol}^{-1}$. $\text{C}_4\text{H}_{30}\text{B}_6\text{N}_2\text{NiO}_{19}$. Anal. Calc.: C = 9.0%, H = 5.7%, N = 5.2%. Found: C = 9.3%, H = 5.5%, N = 5.5. ^{11}B /ppm: 15.8. IR (KBr/ cm^{-1}): 3399(s), 1642(m), 1416(s), 1355(s), 1247(s), 1120(s), 1052(m), 1009(m), 962(m), 859(m), 813(s), 700(m). sc-XRD crystal data: $M_r = 533.87$, triclinic, $P-1$ (No. 2), $a = 9.1508(4) \text{ \AA}$, $b = 9.8599(4) \text{ \AA}$, $c = 13.5971(4) \text{ \AA}$, $\alpha = 88.525(3)^\circ$, $\beta = 70.627(3)^\circ$, $\gamma = 65.245(4)^\circ$, $V = 1041.79(8) \text{ \AA}^3$, $T = 100(2) \text{ K}$, $Z = 2$, $Z' = 1$, $\mu(\text{MoK}\alpha) = 1.023 \text{ mm}^{-1}$, 15537 reflections measured, 4713 unique ($R_{\text{int}} = 0.0461$) which were used in all calculations. The final wR_2 was 0.1048 (all data) and R_1 was 0.0403 ($I > 2\sigma(I)$).

4. Conclusions

Eight new oxidoborate $\text{Ni}(\text{II})$ compounds were prepared by self-assembly crystallization processes from aqueous solution starting from $\text{B}(\text{OH})_3$ and selected $\text{Ni}(\text{II})$ complexes. Six of these compounds were salts containing *insular* oxidoborate anions, but two products were complexes containing *coordinated* oxidoborate(2-) anions, with energetically favourable Ni-O bonds. The two products that contained coordinated hexaborate(2-) ligands were neutral monomeric complexes, rather than the 1-D coordination polymers that we have occasionally observed in related $\text{Cu}(\text{II})$ and $\text{Zn}(\text{II})$ chemistry. The new compounds were templated in all cases by numerous strong structure-directing inter/intramolecular H-bonding interactions involving the oxidoborate ligands and many novel H-bonding motifs are noted and described. This work further demonstrates that in general the inclusion of labile metal complexes into aqueous solutions containing $\text{B}(\text{OH})_3$ can lead to the self-assembly of novel species including those with coordinated oxidoborate ligands and that this synthetic strategy could be applied successfully to other systems.

Supplementary Materials: The following are available online at <https://www.mdpi.com/article/10.3390/inorganics9090068/s1>: single-crystal XRD data, including H-bond interactions.

Author Contributions: M.A.B. conceived the experiments; M.A.A. synthesized and characterized the complexes and grew the single-crystals; P.N.H. and S.J.C. solved the crystal structures; M.A.B. wrote the paper with contributions from all co-authors. All authors have read and agreed to the published version of the manuscript.

Funding: This research received no external funding.

Institutional Review Board Statement: Not applicable.

Informed Consent Statement: Not applicable.

Data Availability Statement: Crystallographic data available from CCDC, UK, see Section 3.2 for details.

Acknowledgments: We thank the EPSRC for the use of the X-ray Crystallographic Service (NCS, Southampton, UK).

Conflicts of Interest: The authors declare no conflict of interest.

References

1. Beckett, M.A.; Brellocks, B.; Chizhevsky, I.T.; Damhus, T.; Hellwich, K.-H.; Kennedy, J.D.; Laitinen, R.; Powell, W.H.; Rabinovich, D.; Vinas, C.; et al. Nomenclature for boranes and related species (IUPAC Recommendations 2019). *Pure Appl. Chem.* **2020**, *92*, 355–381. [[CrossRef](#)]
2. Heller, G. A survey of structural types of borates and polyborates. *Top. Curr. Chem.* **1986**, *131*, 39–98.
3. Grice, J.D.; Burns, P.C.; Hawthorne, F.C. Borate minerals II. A hierarchy of structures based upon the borate fundamental building block. *Canad. Min.* **1999**, *37*, 731–762.

4. Christ, C.L.; Clark, J.R. A crystal-chemical classification of borate structures with emphasis on hydrated borates. *Phys. Chem. Miner.* **1977**, *2*, 59–87. [[CrossRef](#)]
5. Beckett, M.A. Recent Advances in crystalline hydrated borates with non-metal or transition-metal complex cations. *Coord. Chem. Rev.* **2016**, *323*, 2–14. [[CrossRef](#)]
6. Schubert, D.M. Borates in industrial use. *Struct. Bond.* **2003**, *105*, 1–40.
7. Schubert, D.M. Boron oxide, boric acid, and borates. In *Kirk-Othmer Encyclopedia of Chemical Technology*, 5th ed.; John and Wiley and Sons: Hoboken, NJ, USA, 2011; pp. 1–68.
8. Schubert, D.M. Hydrated zinc borates and their industrial use. *Molecules* **2019**, *24*, 2419. [[CrossRef](#)] [[PubMed](#)]
9. Li, P.; Li, L.-Q.; Huang, H.-S.; Liu, Z.-H. Solvothermal synthesis and crystal structures of two novel borates $[(\text{CH}_3)_3\text{NH}][\text{B}_5\text{O}_6(\text{OH})_4]$ and $\text{Na}_2[\text{H}_2\text{TMED}][\text{B}_7\text{O}_9(\text{OH})_5]_2$. *J. Clust. Sci.* **2014**, *25*, 893–903. [[CrossRef](#)]
10. Liang, J.; Wang, Y.-G.; Wang, Y.-X.; Liao, F.-H.; Lin, J.-H. Supramolecular assembly of borate with quaternary ammonium: Crystal structure and tunable luminescent properties. *J. Solid State Chem.* **2013**, *200*, 99–104. [[CrossRef](#)]
11. Jemai, N.; Rzaigui, M.; Akriche, S. Stabilization of hexaborate nets with mixed Co(II) metal and organic cations: Synthesis, rationale, characterization, comparative study and enhancement of bioactivity. *J. Clus. Sci.* **2015**, *26*, 2051–2064. [[CrossRef](#)]
12. Becker, P. Borate materials in nonlinear optics. *Adv. Mater.* **1998**, *10*, 979–992. [[CrossRef](#)]
13. Wang, Y.; Pan, S. Recent developments of metal borate halides: Crystal chemistry and application in second-order NLO materials. *Coord. Chem. Rev.* **2016**, *323*, 15–35. [[CrossRef](#)]
14. Becker, P.; Held, P.; Bohaty, L. Crystal growth and optical properties of the polar hydrated pentaborates $\text{Rb}[\text{B}_5\text{O}_6(\text{OH})_4] \cdot 2\text{H}_2\text{O}$ and $\text{NH}_4[\text{B}_5\text{O}_6(\text{OH})_4] \cdot 2\text{H}_2\text{O}$ and structure redetermination of the ammonium compound. *Cryst. Res. Technol.* **2000**, *35*, 1251–1262. [[CrossRef](#)]
15. Liu, H.-X.; Liang, Y.-X.; Jiang, X. Synthesis, crystal structure and NLO properties of a nonmetal pentaborate $[\text{C}_6\text{H}_{13}\text{N}_2][\text{B}_5\text{O}_6(\text{OH})_4]$. *J. Solid State Chem.* **2008**, *181*, 3243–3247. [[CrossRef](#)]
16. Beckett, M.A.; Coles, S.J.; Horton, P.N.; Jones, C.L.; Krueger, K. Synthesis, XRD studies and NLO properties of $[p\text{-H}_2\text{NC}_6\text{H}_4\text{CH}_2\text{NH}_3][\text{B}_5\text{O}_6(\text{OH})_4] \cdot 2\text{H}_2\text{O}$ and NLO properties of some related salts. *J. Clus. Sci.* **2017**, *28*, 2087–2095. [[CrossRef](#)]
17. Yang, S.; Li, G.; Tian, S.; Liao, F.; Lin, J. Synthesis and structure of $[\text{C}_2\text{H}_{10}\text{N}_2][\text{B}_5\text{O}_8(\text{OH})]$: A nonmetal pentaborate with nonlinear optical properties. *J. Cryst. Growth Des.* **2007**, *7*, 1246–1250. [[CrossRef](#)]
18. Paul, A.K.; Sachidananda, K.; Natarajan, S. $[\text{B}_4\text{O}_9\text{H}_2]$ cyclic borates as the building unit in a family of zinc borate structures. *Cryst. Growth Des.* **2010**, *10*, 456–464. [[CrossRef](#)]
19. Salentine, G. High-field ^{11}B NMR of alkali borate. Aqueous polyborate equilibria. *Inorg. Chem.* **1983**, *22*, 3920–3924. [[CrossRef](#)]
20. Anderson, J.L.; Eyring, E.M.; Whittaker, M.P. Temperature jump rate studies of polyborate formation in aqueous boric acid. *J. Phys. Chem.* **1964**, *68*, 1128–1132. [[CrossRef](#)]
21. Corbett, P.T.; Leclaire, J.; Vial, L.; West, K.R.; Wietor, J.-L.; Sanders, J.K.M.; Otto, S. Dynamic combinatorial chemistry. *Chem. Rev.* **2006**, *106*, 3652–3711. [[CrossRef](#)]
22. Sola, J.; Lafuente, M.; Atcher, J.; Alfonso, I. Constitutional self-selection from dynamic combinatorial libraries in aqueous solution through supramolecular interactions. *Chem. Commun.* **2014**, *50*, 4564–4566. [[CrossRef](#)]
23. Dunitz, J.D.; Gavezzotti, A. Supramolecular synthons: Validation and ranking of intermolecular interaction energies. *Cryst. Growth Des.* **2012**, *12*, 5873–5877. [[CrossRef](#)]
24. Desiraju, G.R. Supramolecular synthons in crystal engineering—A new organic synthesis. *Angew. Chem. Int. Ed. Engl.* **1995**, *34*, 2311–2327. [[CrossRef](#)]
25. Wiebcke, M.; Freyhardt, C.C.; Felsche, J.; Engelhardt, G. Clathrates with three-dimensional host structures of hydrogen bonded pentaborate $[\text{B}_5\text{O}_6(\text{OH})_4]^-$ ions: Pentaborates with the cations NMe_4^+ , NEt_4^+ , NPhMe_3^+ and pipH^+ ($\text{pipH}^+ = \text{piperidinium}$). *Z. Naturforsch.* **1993**, *48*, 978–985. [[CrossRef](#)]
26. Visi, M.Z.; Knobler, C.B.; Owen, J.J.; Khan, M.I.; Schubert, D.M. Structures of self-assembled nonmetal borates derived from α, ω -diaminoalkanes. *Cryst. Growth Des.* **2006**, *6*, 538–545. [[CrossRef](#)]
27. Beckett, M.A.; Coles, S.J.; Davies, R.A.; Horton, P.N.; Jones, C.L. Pentaborate(1-) salts templated by substituted pyrrolidinium cations: Synthesis, structural characterization, and modelling of solid-state H-bond interactions by DFT calculations. *Dalton Trans.* **2015**, *44*, 7032–7040. [[CrossRef](#)]
28. Beckett, M.A.; Coles, S.J.; Horton, P.N.; Jones, C.L. Polyborate anions partnered with large nonmetal cations: Triborate(1-) pentaborate(1-) and heptaborate(2-) salts. *Eur. J. Inorg. Chem.* **2017**, 4510–4518. [[CrossRef](#)]
29. Altahan, M.A.; Beckett, M.A.; Coles, S.J.; Horton, P.N. A new polyborate anion $[\text{B}_7\text{O}_9(\text{OH})_6]^{3-}$: Self-assembly, XRD and thermal properties of *s-fac*- $[\text{Co}(\text{en})_3][\text{B}_7\text{O}_9(\text{OH})_6] \cdot 9\text{H}_2\text{O}$. *Inorg. Chem. Commun.* **2015**, *59*, 95–98. [[CrossRef](#)]
30. Altahan, M.A.; Beckett, M.A.; Coles, S.J.; Horton, P.N. A new decaoxidoctaborate(2-) anion, $[\text{B}_8\text{O}_{10}(\text{OH})_6]^{2-}$: Synthesis and characterization of $[\text{Co}(\text{en})_3][\text{B}_5\text{O}_6(\text{OH})_4][\text{B}_8\text{O}_{10}(\text{OH})_6] \cdot 5\text{H}_2\text{O}$ ($\text{en} = 1,2\text{-diaminoethane}$). *Inorg. Chem.* **2015**, *54*, 412–414. [[CrossRef](#)]
31. Taube, H. Rates and mechanisms of substitutions in inorganic complexes in aqueous solution. *Chem. Rev.* **1952**, *50*, 69–126. [[CrossRef](#)]

32. Altahan, M.A.; Beckett, M.A.; Coles, S.J.; Horton, P.N. Transition-metal complexes with oxidoborates. Synthesis and XRD characterization of $[\text{H}_3\text{NCH}_2\text{CH}_2\text{NH}_2]\text{Zn}\{\text{k}^3\text{O}, \text{O}', \text{O}''\text{-B}_{12}\text{O}_{18}(\text{OH})_6\text{-k}^1\text{O}'''\}$ $\text{Zn}(\text{en})(\text{NH}_2\text{CH}_2\text{CH}_2\text{NH}_3)]\cdot 8\text{H}_2\text{O}$: A neutral bimetallic zwitterionic polyborate system containing the 'isolated' dodecaborate(6-) anion. *Pure Appl. Chem.* **2018**, *90*, 625–632. [[CrossRef](#)]
33. Altahan, M.A.; Beckett, M.A.; Coles, S.J.; Horton, P.N. Oxidopolyborate anions templated by transition-metal complexes: Self-assembled synthesis and structural studies (XRD) of $[\text{Co}(\text{NH}_3)_6]\text{[B}_4\text{O}_5(\text{OH})_4\text{]}_3\cdot 11\text{H}_2\text{O}$, $[\text{Ni}(\text{phen})_3]\text{[B}_7\text{O}_9(\text{OH})_5\text{]}\cdot 9.5\text{H}_2\text{O}$ and $[\text{Zn}(\text{dac})_2(\text{H}_2\text{O})_2]\text{[B}_7\text{O}_9(\text{OH})_5\text{]}\cdot \text{H}_2\text{O}$. *J. Mol. Struct.* **2020**, *1200*, 127071. [[CrossRef](#)]
34. Altahan, M.A.; Beckett, M.A.; Coles, S.J.; Horton, P.N. Two 1-D Coordination Polymers containing Zinc(II) Hexaborates: $[\text{Zn}(\text{en})\{\text{B}_6\text{O}_7(\text{OH})_6\}]\cdot 2\text{H}_2\text{O}$ (en = 1,2-diaminoethane) and $[\text{Zn}(\text{pn})\{\text{B}_6\text{O}_7(\text{OH})_6\}]\cdot 1.5\text{H}_2\text{O}$ (pn = (+/−) 1,2-diaminopropane). *Crystals* **2018**, *8*, 470. [[CrossRef](#)]
35. Altahan, M.A.; Beckett, M.A.; Coles, S.J.; Horton, P.N. Hexaborate(2-) and dodecaborate(12-) anions as ligands to zinc(II) centres: Self-assembly and single crystal XRD characterization of $[\text{Zn}\{\text{k}^3\text{O-B}_6\text{O}_7(\text{OH})_6\}(\text{k}^3\text{-N-dien})]0.5\text{H}_2\text{O}$ (dien = $\text{NH}(\text{CH}_2\text{CH}_2\text{NH}_2)_2$), $(\text{NH}_4)_2[\text{Zn}\{\text{k}^2\text{-O-B}_6\text{O}_7(\text{OH})_6\}(\text{H}_2\text{O})_2]\cdot 2\text{H}_2\text{O}$ and $(1,3\text{-pn})_3\{[\text{k}^1\text{-NH}_3\{\text{CH}_2\}_3\text{NH}_2]\text{Zn}\{\text{k}^3\text{-O-B}_{12}\text{O}_{18}(\text{OH})_6\}\}_2\cdot 14\text{H}_2\text{O}$. *Inorganics* **2019**, *7*, 44. [[CrossRef](#)]
36. Altahan, M.A.; Beckett, M.A.; Coles, S.J.; Horton, P.N. Oxidoborate chemistry: The self-assembled, templated, synthesis, and an XRD study of a 1-D coordination polymer $[\text{Cu}(\text{en})\{\text{B}_6\text{O}_7(\text{OH})_6\}]\cdot 3\text{H}_2\text{O}$ (en = 1,2-diaminoethane). *Phosphorus Sulfur Silicon Relat. Elem.* **2020**, *195*, 952–956. [[CrossRef](#)]
37. Altahan, M.A.; Beckett, M.A.; Coles, S.J.; Horton, P.N. Synthesis and characterization of polyborates templated by cationic copper(II) complexes: Structural (XRD), spectroscopic, thermal (TGA/DSC) and magnetic properties. *Polyhedron* **2017**, *135*, 247–257. [[CrossRef](#)]
38. Altahan, M.A.; Beckett, M.A.; Coles, S.J.; Horton, P.N. Copper(2+) complexes of hydroxyoxidoborates. Synthesis and characterization of two clusters containing the hexaborate(2-) ligand: $[\text{Cu}(\text{NH}_2\text{CH}_2\text{CH}_2\text{NEt}_2)\{\text{B}_6\text{O}_7(\text{OH})_6\}]\cdot 5\text{H}_2\text{O}$ and $[\text{Cu}(\text{NH}_3)_2\{\text{B}_6\text{O}_7(\text{OH})_6\}]\cdot 2\text{H}_2\text{O}$. *J. Cluster Sci.* **2019**, *30*, 599–605. [[CrossRef](#)]
39. Altahan, M.A.; Beckett, M.A.; Coles, S.J.; Horton, P.N. Synthesis and characterization by a single-crystal XRD study of $[\text{H}_3\text{O}]_4[\text{Cu}_7(\text{NH}_3)_2(\text{H}_2\text{O})_4\{\text{B}_{24}\text{O}_{39}(\text{OH})_{12}\}]\cdot 13\text{H}_2\text{O}$: An unusual bis(hydroxytrioxidodiborate) tri-metallic chain supported by a $[\{\text{Cu}_4\text{O}\}\{\text{B}_{20}\text{O}_{32}(\text{OH})_8\}]^{6-}$ cluster. *J. Cluster Sci.* **2018**, *29*, 1337–1343. [[CrossRef](#)]
40. Altahan, M.A.; Beckett, M.A.; Coles, S.J.; Horton, P.N. Copper(2+) complexes of hydroxyoxido polyborates: Synthesis and characterization of $[\text{Cu}(\text{MeNHCH}_2\text{CH}_2\text{NMeH}_2)(\text{H}_2\text{O})_2]\text{[B}_5\text{O}_6(\text{OH})_4\text{]}_2\cdot 2\text{B}(\text{OH})_3$. *Phosphorus Sulfur Silicon Relat. Elem.* **2019**, *194*, 948–951. [[CrossRef](#)]
41. Lan, S.M.; Di, W.-J.; Shao, Z.-D.; Liang, Y.-X. Two new transition metal inorganic–organic hybrid borates: [tris(2-aminoethoxy)trihydroxyhexaborato]cobalt(II) and its nickel(II) analogue. *Acta Cryst.* **2011**, *C67*, m338–m341. [[CrossRef](#)]
42. Zheng, L.; Zhang, J.; Liu, Z. Synthesis, crystal structures and thermal behavior of $\text{Co}(\text{en})_3\text{[B}_4\text{O}_5(\text{OH})_4\text{]Cl}\cdot 3\text{H}_2\text{O}$ and $[\text{Ni}(\text{en})_3]\text{[B}_5\text{O}_6(\text{OH})_4\text{]}\cdot 2\text{H}_2\text{O}$. *J. Chin. Chem.* **2009**, *27*, 494–500. [[CrossRef](#)]
43. Pan, C.-Y.; Hu, S.; Li, D.-G.; Ouyang, P.; Zhao, F.-H.; Zheng, Y.-Y. The first ferroelectric templated borate: $[\text{Ni}(\text{en})_2\text{pip}]\text{[B}_5\text{O}_6(\text{OH})_4\text{]}\cdot 2\text{H}_2\text{O}$. *Dalton Trans.* **2010**, *39*, 5772–5777. [[CrossRef](#)]
44. Liu, Z.-H.; Zhang, J.-J.; Zhang, W.-J. Synthesis, crystal structure and vibrational spectroscopy of a novel mixed ligands Ni(II) pentaborate $[\text{Ni}(\text{C}_4\text{H}_{10}\text{N}_2)(\text{C}_2\text{H}_8\text{N}_2)_2]\text{[B}_5\text{O}_6(\text{OH})_4\text{]}\cdot 2\text{H}_2\text{O}$. *Inorg. Chim. Acta* **2006**, *359*, 519–524. [[CrossRef](#)]
45. Meng, Q.; Wang, G.M.; He, H.; Yang, B.-F.; Yang, G.-Y. Syntheses and Crystal Structures of Two New Pentaborates Templated by Transition-Metal Complexes. *J. Clust. Sci.* **2014**, *25*, 1295–1305. [[CrossRef](#)]
46. Avdeeva, V.V.; Malinina, E.A.; Vologzhanina, A.V.; Sivaev, I.B.; Kuznetsov, N.T. Formation of oxidopolyborates in destruction of the $[\text{B}_{11}\text{H}_{14}]^-$ anion promoted by transition metals. *Inorg. Chim. Acta* **2020**, *509*, 119693. [[CrossRef](#)]
47. Liu, X.; Zhang, F.; Yin, X.H. Hydrothermal synthesis and crystal structure of organic-hybrid borate $[\text{Ni}(\text{dien})_2]\text{[B}_5\text{O}_6(\text{OH})_4\text{]}\cdot 2\text{H}_2\text{O}$. *Chem. Res. Appl.* **2010**, *22*, 1587–1591.
48. Kose, D.A.; Yurdakul, O.; Sahin, O.; Ozturk, Z. The new metal complex templated polyoxoborate(s) (POB(s)) structures. Synthesis, structural characterization, and hydrogen storage capacities. *J. Mol. Struct.* **2017**, *1134*, 806–813. [[CrossRef](#)]
49. Hathaway, B.J.; Hodgson, P.G. Copper-ligand bond-lengths in axial complexes of the copper(II) ion. *J. Inorg. Nucl. Chem.* **1973**, *35*, 4071–4081. [[CrossRef](#)]
50. Liu, Z.-H.; Li, L.-Q.; Zhang, W.-J. Two new borates containing the first examples of large isolated polyborate anions: Chain $[\text{B}_7\text{O}_9(\text{OH})_5]^{2-}$ and Ring $[\text{B}_{14}\text{O}_{20}(\text{OH})_6]^{4-}$. *Inorg. Chem.* **2006**, *45*, 1430–1432. [[CrossRef](#)]
51. Schubert, D.M.; Visi, M.Z.; Khan, S.; Knobler, C.B. Synthesis and structure of a new heptaborate oxoanion isomer: $\text{B}_7\text{O}_9(\text{OH})_5^{2-}$. *Inorg. Chem.* **2008**, *47*, 4740–4745. [[CrossRef](#)] [[PubMed](#)]
52. Beckett, M.A.; Horton, P.N.; Hursthouse, M.B.; Timmis, J.L.; Varma, K.S. Templated heptaborate and pentaborate salts of cyclo-alkylammonium cations: Structural and thermal properties. *Dalton Trans.* **2012**, *41*, 4396–4403. [[CrossRef](#)]
53. Sacconi, L.; Mani, F.; Bencini, A. Nickel. In *Comprehensive Coordination Chemistry*; Wilkinson, G., Gillard, R.D., McCleverty, J.A., Eds.; Pergamon Books Ltd.: Oxford, UK, 1987; Volume 5, Chapter 50; pp. 1–347.
54. Ihara, Y.; Satake, Y.; Fujimolo, Y.; Senda, H.; Suzuki, M.; Uehara, A. X-ray structures of octahedral diaqua(N,N)dialkylethelenediamine nickel(II) complexes possessing elongated nickel(II)-nitrogen bonds along axial direction. *Bull. Chem. Soc. Jpn.* **1991**, *64*, 2349–2352. [[CrossRef](#)]
55. Zhou, J.; Yin, X.-H.; Zhang, F. Two novel thioindate-thioantimonate compounds with $[\text{Ni}(\text{dien})_2]\text{In}_2\text{Sb}_4\text{S}_{11}$ and $[\text{Ni}(\text{dien})_2](\text{In}_3\text{Sb}_2\text{S}_9)_2\cdot 2\text{H}_2\text{O}$ with transition metal complexes. *Inorg. Chem.* **2010**, *49*, 9671–9676. [[CrossRef](#)]

56. Natarajan, S.; Klein, W.; Panthoefler, M.; Wuellen, L.V.; Jansen, M. Solution mediated synthesis and structure of the first anionic bis(hexaborato)-zincate prepared in the presence of organic base. *Z. Anorg. Allg. Chem.* **2003**, *629*, 959–962. [[CrossRef](#)]
57. Jemai, N.; Rzaigui, S.; Akriche, S. Piperazine-1,4-dium bis(hexahydroxidoheptaoxidohexaborato- k^3O,O',O'')cobaltate(II) hexahydrate. *Acta Cryst.* **2014**, *70*, m167–m169. [[CrossRef](#)]
58. Xin, S.-S.; Zhou, M.-H.; Beckett, M.A.; Pan, C.-Y. Recent advances in crystalline oxidoborate complexes of *d*-block or *p*-block metals: Structural aspects, syntheses and physical properties. *Molecules* **2021**, *26*, 3815. [[CrossRef](#)]
59. Etter, M.C. Encoding and decoding hydrogen-bond patterns of organic chemistry. *Acc. Chem. Res.* **1990**, *23*, 120–126. [[CrossRef](#)]
60. Zolotarev, P.N.; Arshad, M.N.; Asiri, A.M.; Al-amshany, Z.M.; Blatov, V.A. A possible route toward expert systems in supramolecular chemistry: 2-periodic H-bonded patterns in molecular crystals. *Cryst. Growth Des.* **2014**, *14*, 1938–1949. [[CrossRef](#)]
61. Figgis, B.N.; Lewis, J. The magnetic properties of transition metal complexes. *Prog. Inorg. Chem.* **1964**, *6*, 37–239. [[CrossRef](#)]
62. Elfring, W.H.; Rose, N.J. Studies of three nickel(II) containing different macrocyclic ligands derived from acetylacetone and triethylenetetramine. *Inorg. Chem.* **1975**, *14*, 2759–2768. [[CrossRef](#)]
63. Li, J.; Xia, S.; Gao, S. FT-IR and Raman spectroscopic study of hydrated borates. *Spectrochim. Acta* **1995**, *51*, 519–532. [[CrossRef](#)]
64. Beckett, M.A.; Horton, P.N.; Coles, S.J.; Kose, D.A.; Kreuziger, A.-M. Structural and thermal studies of non-metal cation pentaborate salts derived from 1,5-diazobicyclo[4.3.0]non-5-ene, 1,8-diazobicyclo[5.4.0]undec-7-ene and 1,8-bis(dimethylamino)naphthalene. *Polyhedron* **2012**, *38*, 157–161. [[CrossRef](#)]
65. Breckenridge, J.G. Copper(II) and nickel(II) coordination compounds with diethyltriamine and hydroxyethylethylenediamine ligands. *Can. J. Res.* **1948**, *6*, 11–19. [[CrossRef](#)]
66. Cui, A.; Chen, X.; Sun, J.; Wei, J.; Yang, J.; Kou, H. Preparation and thermochromic properties of copper(II)-*N,N*-diethylethylenediamine. *J. Chem Educ.* **2011**, *88*, 311–312. [[CrossRef](#)]
67. Wendlandt, W.W. The thermal decomposition of metal complexes—VI. Some amine complexes of copper(II) sulphate. *J. Inorg. Nucl. Chem.* **1963**, *25*, 833–842. [[CrossRef](#)]
68. Saito, R.; Kidani, Y. Preparative separation of *cis*- and *trans*-1,2-diaminocyclohexane by means of selective nickel(II) complex formation. *Chem. Lett.* **1976**, *5*, 123–126. [[CrossRef](#)]
69. *CrysAlis Pro Software System*; Applied Rigaku Technologies, Inc.: Austin, TX, USA, 2021.
70. *CrystalClear-SM*; Expert 2.1 Software; Applied Rigaku Technologies, Inc.: Austin, TX, USA, 2013.
71. Dolomanov, O.V.; Bourhis, L.J.; Gildea, R.J.; Howard, J.A.K.; Puschmann, H. Olex2: A complete structure solution, refinement, and analysis programme. *J. Appl. Cryst.* **2009**, *42*, 339–341. [[CrossRef](#)]
72. Sheldrick, G.M. ShelXT-intergrated space-group and crystal-structure determination. *Acta Crystallogr. Sect. A Found. Adv.* **2015**, *71*, 3–8. [[CrossRef](#)]
73. Sheldrick, G.M. Crystal structure refinement with SHELXL. *Acta Crystallogr. Sect. C Struct. Chem.* **2015**, *71*, 3–8. [[CrossRef](#)] [[PubMed](#)]